

# Spin-flip process through a quantum dot coupled to ferromagnetic electrodes

Huanwen Lai, Xuean Zhao, Zhu-An Xu, and You-Quan Li

*Zhejiang Institute of Modern Physics and Department of Physics, Zhejiang University, Hangzhou 310027, China*

---

## Abstract

We study the spin-dependent transport through a quantum dot coupled to two ferromagnetic electrodes using the equation of motion method for the nonequilibrium Green's functions. Our results show that the conductance and the density of states (DOS) are strongly dependent on the configurations of the magnetic electrodes. In parallel configuration of magnetic electrodes the conductance is affected by the spin-flip process and the Coulomb repulsion on the dot. The Kondo peak for spin-dependent transport is splitted into two peaks by the spin-flip process. The locations of the two peaks are symmetric about no spin-flip peak and the separation of the splitting is dependent on the strength of the spin-flip parameter  $R$ . This effect may be useful to realize the spin-filter device.

*Key words:* Green's function, quantum dot, spin-flip, Kondo effect

*PACS:* 73.23.-b, 74.25.Fy, 75.25.+z

---

## 1 Introduction

In metallic bulk the dilute magnetic impurities are screened by the itinerant electron spins and cause anomalous resonant scattering of conducting electrons[1]. It shows up a minimum in electric resistivity at the low temperature. In the past decade Kondo phenomena in quantum dots coupled to metallic leads has attracted much attention[2,3,4,5,6,7,8] and has been studied intensively in both theories and experiments. There is a fundamental difference between the Kondo effect in quantum dots and the Kondo effect in alloys with magnetic impurities. In the latter case the dressed localized magnetic moment increases the scattering cross section and as a result there is a minimum in the resistivity, whereas for the former case the resistivity depends on the parity of the level occupied by electrons. However, the physics responsible for these

resistances is similar. In both cases the effect is due to the spin correlated transport at the Fermi level.

The Kondo effect has been understood in the structure that a quantum dot coupled to the normal electrodes in equilibrium and out of equilibrium[9,10,11,12,13,14,15,16,17,18]. It is a consequence of high order perturbation and co-tunnelling process caused by the electron-spin interaction between electrons in the quantum dot and in lead. The Kondo effect through quantum dots coupled to external leads can even induce current in the Coulomb blockade regime by making spin correlated singlet and triplet with electron spins outside the quantum dot[3,4]. The conductance is related to the number of electrons in the dot. Usually the Kondo effect appears when the dot has odd number of electrons (total spin 1/2), but is absent when the dot has even number of electrons (total spin 0). The conductance or the density of states (DOS) of the dot is enhanced by the Kondo effect at low temperature. However, for the ferromagnetic-quantum dot-ferromagnetic system, the question is open. We want to know what is the manifestations of the Kondo effect when the magnetic moments of the electrodes are taken into account in finite and infinite Coulomb repulsion.

In this work, we investigate the spin-dependent transport in an interacting quantum dot coupled to two ferromagnetic electrodes. Different from the conventional Kondo problem in normal electrodes, i.e., quantum dot-normal electrodes system, here we deal with the strong electronic correlation, which is sensitive to the relative orientations of magnetization between the two electrodes. The paper is organized as follows. In Sec. 2 we describe the model of the system and then calculate the nonequilibrium Green's functions using the equation of motion method. The general expression for the electric current flowing through the dot in terms of nonequilibrium Green's functions is given. In Sec. 3 we present numerical results with and without the spin-flip process in the dot for the arbitrary Coulomb repulsion  $U$ . We have some conclusions in Sec. 4.

## 2 Model

The Hamiltonian for the quantum dot coupled to two ferromagnetic electrodes reads

$$H = \sum_{k;\alpha \in L,R;\sigma} \varepsilon_{k\alpha\sigma} a_{k\alpha\sigma}^+ a_{k\alpha\sigma} + \sum_{\sigma} \varepsilon_d d_{\sigma}^+ d_{\sigma} + U d_{\uparrow}^+ d_{\uparrow} d_{\downarrow}^+ d_{\downarrow} + R(d_{\uparrow}^+ d_{\downarrow} + d_{\downarrow}^+ d_{\uparrow}) + \sum_{k;\alpha \in L,R;\sigma} (V_{k\sigma} a_{k\alpha\sigma}^+ d_{\sigma} + h.c.). \quad (1)$$

Here the single-particle energy  $\varepsilon_d$  in quantum dot is double degenerate in the spin index  $\sigma$  ( $\sigma=\uparrow\downarrow, \pm$ ), and the Coulomb repulsion interaction in the dot is  $U$ . The first term in Hamiltonian describes the free electron in magnetic electrodes, the second and third terms represent the correlated level of the quantum dot, the fourth term is to describe spin-orbit coupling which may cause the spin rotation of an electron in the quantum dot, and the last term is the spin-dependent hybridization of the quantum dot with the magnetic electrodes.

Since the spin quantization axes in the electrodes are fixed by the internal magnetization of the magnets, an electron is in a superposition of spin-up and spin-down states as it tunnels into and out the dot. In calculations we have to take into account the coherent processes. Technically, we take a transformation[18,19],

$$d_\sigma = \frac{1}{\sqrt{2}}(c_\sigma - \sigma c_{\bar{\sigma}}). \quad (2)$$

In terms of Eq. (2) the Hamiltonian becomes

$$H = \sum_{k;\alpha \in L,R;\sigma} \varepsilon_{k\alpha\sigma} a_{k\alpha\sigma}^\dagger a_{k\alpha\sigma} + \sum_{\sigma} \varepsilon_{c\sigma} c_{\sigma}^\dagger c_{\sigma} + U c_{\uparrow}^\dagger c_{\uparrow} c_{\downarrow}^\dagger c_{\downarrow} \\ + \sum_{k;\alpha \in L,R;\sigma} \left( \frac{1}{\sqrt{2}} V_{k\sigma} a_{k\alpha\sigma}^\dagger c_{\sigma} - \frac{\sigma}{\sqrt{2}} V_{k\alpha\sigma}^* a_{k\alpha\sigma}^\dagger c_{\bar{\sigma}} + h.c. \right), \quad (3)$$

where  $\varepsilon_{c\sigma} = \varepsilon_d + \sigma R$  for spin- $\sigma$ . The current through the left electrode can be calculated in terms of nonequilibrium Green's functions with the tunnelling matrix

$$\mathbf{V}_{k\alpha} = \frac{1}{\sqrt{2}} \begin{pmatrix} V_{k\alpha\uparrow} & V_{k\alpha\downarrow} \\ -V_{k\alpha\uparrow} & V_{k\alpha\downarrow} \end{pmatrix}. \quad (4)$$

The current is

$$J = \frac{2e}{\hbar} \text{Re} \sum_k \int \text{Tr}[\mathbf{V}_{kL} \mathbf{G}_{kL}^<(\omega)], \quad (5)$$

where  $[\mathbf{G}_{kL}^<(t)]_{\sigma\sigma'} = i \langle a_{kL\sigma}^\dagger(0), c_{\sigma'}(t) \rangle$  is the less Green's function of the left electrode.

Now we apply Dyson's equation to express the current  $J$  by the Green's func-

tions  $\mathbf{G}$  of the dot,

$$J = \frac{ie}{\hbar} \int \frac{d\epsilon}{2\pi} Tr\{\mathbf{\Gamma}^L(\omega) \mathbf{G}^<(\omega) + f_L(\epsilon)[\mathbf{G}^R(\omega) - \mathbf{G}^A(\omega)]\}, \quad (6)$$

where the less Green's function of the dot  $[\mathbf{G}^<(\omega)]_{\sigma\sigma'} = i\langle c_{\sigma'}^+(t), c_{\sigma}(0) \rangle$ . The retarded (advanced) Green's function of the dot  $[\mathbf{G}^{R(A)}(\omega)]_{\sigma\sigma'} = \mp i\langle \{c_{\sigma}(t), c_{\sigma'}^+(0)\} \rangle$ , respectively. The upper sign is for retarded Green's function and the lower sign is for advanced Green's function.  $f_{\alpha}(\epsilon)$  is the Fermi distribution function in the  $\alpha$  electrode, and

$$\mathbf{\Gamma}^{\alpha}(\omega) = \frac{1}{2} \begin{pmatrix} \Gamma_{\uparrow}^{\alpha}(\omega) + \Gamma_{\downarrow}^{\alpha}(\omega) & \Gamma_{\downarrow}^{\alpha}(\omega) - \Gamma_{\uparrow}^{\alpha}(\omega) \\ \Gamma_{\downarrow}^{\alpha}(\omega) - \Gamma_{\uparrow}^{\alpha}(\omega) & \Gamma_{\uparrow}^{\alpha}(\omega) + \Gamma_{\downarrow}^{\alpha}(\omega) \end{pmatrix} \quad (7)$$

is the linewidth matrix with  $\Gamma_{\sigma}^{\alpha}(\omega) = 2\pi \sum_k |V_{k\alpha\sigma}|^2 \delta(\omega - \varepsilon_{k\alpha\sigma})$ . The spin dependence of  $\Gamma_{\sigma}^{\alpha}(\epsilon)$  originates from the bulk magnetization of the electrodes.

In order to determine the current  $J$ , we should first determine the Green's function of the dot. As we know the retarded Green's function  $\mathbf{G}^R$  is a conjugation of the advanced Green's function  $\mathbf{G}^A$ , we need only to calculate  $\mathbf{G}^R$ . With the notation as usual  $G_{\sigma\sigma'}^R \equiv \ll c_{\sigma}, c_{\sigma'}^+ \gg \equiv -i \int_0^{\infty} e^{i\omega t} \langle \{c_{\sigma}(t), c_{\sigma'}^+(0)\} \rangle dt$ , we apply the equation of motion method again to calculate the Green's function  $G_{\sigma\sigma'}^R$ . The first equation of motion for the retarded Green's function  $G_{\sigma\sigma'}^R$  is

$$\omega \ll c_{\sigma}, c_{\sigma'}^+ \gg = \langle \{c_{\sigma}, c_{\sigma'}^+\} \rangle + \ll [c_{\sigma}, H], c_{\sigma'}^+ \gg. \quad (8)$$

Using the Eq. (8),  $G_{\sigma\sigma'}^R$  can be written as

$$(\omega - \varepsilon_{c\sigma})G_{\sigma\sigma'}^R = \delta_{\sigma\sigma'} + U G_{\sigma\sigma'}^{(2)} + \sum_{k;\alpha} \frac{1}{\sqrt{2}} V_{k\alpha\sigma}^* \Gamma_{k\alpha}^{\sigma\sigma'} - \sum_{k;\alpha} \frac{\bar{\sigma}}{\sqrt{2}} V_{k\alpha\bar{\sigma}}^* \Gamma_{k\alpha}^{\bar{\sigma}\sigma'}, \quad (9)$$

where the second order function  $G_{\sigma\sigma'}^{(2)}$ ,  $\Gamma_{k\alpha}^{\sigma\sigma'}$  and  $\Gamma_{k\alpha}^{\bar{\sigma}\sigma'}$  are  $G_{\sigma\sigma'}^{(2)} = \ll c_{\sigma} c_{\bar{\sigma}}^+ c_{\bar{\sigma}}, c_{\sigma'}^+ \gg$ ,  $\Gamma_{k\alpha}^{\sigma\sigma'} = \ll a_{k\alpha\sigma}, c_{\sigma'}^+ \gg$ , and  $\Gamma_{k\alpha}^{\bar{\sigma}\sigma'} = \ll a_{k\alpha\bar{\sigma}}, c_{\sigma'}^+ \gg$ , respectively.

There are three new Green's functions on the right hand side of Eq.(9). The equation of motion for  $\Gamma_{k\alpha}^{\sigma\sigma'}$  and  $\Gamma_{k\alpha}^{\bar{\sigma}\sigma'}$  are close since the only new Green's functions are  $G_{\sigma\sigma'}^R$  and  $G_{\bar{\sigma}\sigma'}^R$ ,

$$\Gamma_{k\alpha}^{\sigma\sigma'} = \frac{1}{\sqrt{2}} V_{k\alpha\sigma} g_{1\sigma}^r G_{\sigma\sigma'}^R - \frac{\sigma}{\sqrt{2}} V_{k\alpha\sigma} g_{1\sigma}^r G_{\bar{\sigma}\sigma'}^R, \quad (10)$$

$$\Gamma_{k\alpha}^{\bar{\sigma}\sigma'} = \frac{1}{\sqrt{2}} V_{k\alpha\bar{\sigma}} g_{2\bar{\sigma}}^r G_{\bar{\sigma}\sigma'}^R - \frac{\bar{\sigma}}{\sqrt{2}} V_{k\alpha\bar{\sigma}} g_{2\bar{\sigma}}^r G_{\sigma\sigma'}^R, \quad (11)$$

where  $g_{1\sigma}^r = (\omega - \varepsilon_{k\alpha\sigma} + i\omega^+)^{-1}$  and  $g_{2\bar{\sigma}}^r = (\omega - \varepsilon_{k\alpha\bar{\sigma}} + i\omega^+)^{-1}$ . Note that  $g_{1\sigma}^r = g_{2\sigma}^r$ .

However, the equation of motion for the new Green's function  $G_{\sigma\sigma'}^{(2)}$ , which is generated by the Coulomb interaction and involves a two-particle Green's function, is not close. We have to truncate the equations. An approximate solution, valid for temperatures higher than the Kondo temperature[20],  $k_B T_K \simeq (U\Gamma)^{(1/2)} \exp(-\pi|\mu - \epsilon_\alpha|/\Gamma)$ , is obtained by neglecting terms in the equation of motion for  $G_{\sigma\sigma'}^{(2)}$  which involves correlations in the leads[10]. We can write out  $G_{\sigma\sigma'}^{(2)}$  as follows,

$$(\omega - \varepsilon_{c\sigma} - U)G_{\sigma\sigma'}^{(2)} = n_{\bar{\sigma}}\delta_{\sigma\sigma'} + \sum_{k;\alpha} \frac{1}{\sqrt{2}} V_{k\alpha\sigma}^* \Gamma_1^{(2)} - \sum_{k;\alpha} \frac{\bar{\sigma}}{\sqrt{2}} V_{k\alpha\bar{\sigma}}^* \Gamma_2^{(2)} \\ - \sum_{k;\alpha} \frac{1}{\sqrt{2}} V_{k\alpha\bar{\sigma}} \Gamma_3^{(2)} + \sum_{k;\alpha} \frac{\sigma}{\sqrt{2}} V_{k\alpha\sigma}^* \Gamma_4^{(2)} + \sum_{k;\alpha} \frac{1}{\sqrt{2}} V_{k\alpha\bar{\sigma}}^* \Gamma_5^{(2)} \\ - \sum_{k;\alpha} \frac{\sigma}{\sqrt{2}} V_{k\alpha\sigma}^* \Gamma_6^{(2)}, \quad (12)$$

with the new notations:  $\Gamma_1^{(2)} = \ll a_{k\alpha\sigma} c_{\bar{\sigma}}^+ c_{\bar{\sigma}}, c_{\sigma'}^+ \gg$ ,  $\Gamma_2^{(2)} = \ll a_{k\alpha\bar{\sigma}} c_{\bar{\sigma}}^+ c_{\bar{\sigma}}, c_{\sigma'}^+ \gg$ ,  $\Gamma_3^{(2)} = \ll c_\sigma a_{k\alpha\bar{\sigma}}^+ c_{\bar{\sigma}}, c_{\sigma'}^+ \gg$ ,  $\Gamma_4^{(2)} = \ll c_\sigma a_{k\alpha\sigma}^+ c_{\bar{\sigma}}, c_{\sigma'}^+ \gg$ ,  $\Gamma_5^{(2)} = \ll c_\sigma c_{\bar{\sigma}}^+ a_{k\alpha\bar{\sigma}}, c_{\sigma'}^+ \gg$ ,  $\Gamma_6^{(2)} = \ll c_\sigma c_{\bar{\sigma}}^+ a_{k\alpha\sigma}, c_{\sigma'}^+ \gg$ .  $n_{\bar{\sigma}} = \langle c_{\bar{\sigma}}^+ c_{\bar{\sigma}} \rangle$  must be calculated self-consistently[11].

As for  $\Gamma_i^{(2)}$ , we adopt the truncation as Y. Meir et al[9,10] and write out  $\Gamma_i^{(2)}$  explicitly as,

$$\Gamma_1^{(2)} = \frac{1}{\sqrt{2}} V_{k\alpha\sigma} g_{1\sigma}^r G_{\sigma\sigma'}^{(2)} - \frac{\sigma}{\sqrt{2}} V_{k\alpha\sigma} g_{1\sigma}^r f(\varepsilon_{k\alpha\sigma}) G_{\sigma\sigma'}^R, \quad (13)$$

$$\Gamma_2^{(2)} = -\frac{\bar{\sigma}}{\sqrt{2}} V_{k\alpha\bar{\sigma}} g_{2\bar{\sigma}}^r G_{\sigma\sigma'}^{(2)} + \frac{1}{\sqrt{2}} V_{k\alpha\bar{\sigma}} g_{2\bar{\sigma}}^r f(\varepsilon_{k\alpha\bar{\sigma}}) G_{\bar{\sigma}\sigma'}^R, \quad (14)$$

$$\Gamma_3^{(2)} = -\frac{1}{\sqrt{2}} V_{k\alpha\bar{\sigma}}^* g_{3\bar{\sigma}}^r G_{\sigma\sigma'}^{(2)} - \frac{\bar{\sigma}}{\sqrt{2}} V_{k\alpha\bar{\sigma}}^* g_{3\bar{\sigma}}^r G_{\bar{\sigma}\sigma'}^{(2)} + \frac{1}{\sqrt{2}} V_{k\alpha\bar{\sigma}}^* g_{3\bar{\sigma}}^r f(\varepsilon_{k\alpha\bar{\sigma}}) G_{\sigma\sigma'}^R \\ + \frac{\bar{\sigma}}{\sqrt{2}} V_{k\alpha\sigma}^* g_{3\bar{\sigma}}^r f(\varepsilon_{k\alpha\bar{\sigma}}) G_{\bar{\sigma}\sigma'}^R, \quad (15)$$

$$\Gamma_4^{(2)} = \frac{\sigma}{\sqrt{2}} V_{k\alpha\sigma}^* g_{4\sigma}^r G_{\sigma\sigma'}^{(2)} + \frac{1}{\sqrt{2}} V_{k\alpha\sigma}^* g_{4\sigma}^r G_{\bar{\sigma}\sigma'}^{(2)} - \frac{\sigma}{\sqrt{2}} V_{k\alpha\sigma}^* g_{4\sigma}^r f(\varepsilon_{k\alpha\sigma}) G_{\sigma\sigma'}^R \\ - \frac{1}{\sqrt{2}} V_{k\alpha\sigma}^* g_{4\sigma}^r f(\varepsilon_{k\alpha\sigma}) G_{\bar{\sigma}\sigma'}^R, \quad (16)$$

$$\Gamma_5^{(2)} = \frac{1}{\sqrt{2}} V_{k\alpha\bar{\sigma}}^* g_{5\bar{\sigma}}^r G_{\sigma\sigma'}^{(2)} - \frac{1}{\sqrt{2}} V_{k\alpha\bar{\sigma}}^* g_{5\bar{\sigma}}^r f(\varepsilon_{k\alpha\bar{\sigma}}) G_{\sigma\sigma'}^R, \quad (17)$$

$$\Gamma_6^{(2)} = -\frac{\sigma}{\sqrt{2}} V_{k\alpha\sigma} g_{6\sigma}^r G_{\sigma\sigma'}^{(2)} + \frac{\sigma}{\sqrt{2}} V_{k\alpha\sigma} g_{6\sigma}^r f(\varepsilon_{k\alpha\sigma}) G_{\sigma\sigma'}^R, \quad (18)$$

with the notations as  $g_{3\bar{\sigma}}^r = (\omega - \varepsilon_{c\sigma} - \varepsilon_{c\bar{\sigma}} + \varepsilon_{k\alpha\bar{\sigma}} - U + i\omega^+)^{-1}$ ,  $g_{4\sigma}^r = (\omega - \varepsilon_{c\sigma} - \varepsilon_{c\bar{\sigma}} + \varepsilon_{k\alpha\sigma} - U + i\omega^+)^{-1}$ ,  $g_{5\bar{\sigma}}^r = (\omega - \varepsilon_{c\sigma} + \varepsilon_{c\bar{\sigma}} - \varepsilon_{k\alpha\bar{\sigma}} + i\omega^+)^{-1}$ , and  $g_{6\sigma}^r = (\omega - \varepsilon_{c\sigma} + \varepsilon_{c\bar{\sigma}} - \varepsilon_{k\alpha\sigma} + i\omega^+)^{-1}$ . Notice that  $g_{3\sigma}^r = g_{4\sigma}^r$ .

Defining  $\Sigma_{i\sigma} = \sum_{k;\alpha} \frac{1}{2} |V_{k\alpha\sigma}|^2 g_{i\sigma}^r$  and  $\Sigma_{i\sigma}^f = \sum_{k;\alpha} \frac{1}{2} |V_{k\alpha\sigma}|^2 f(\varepsilon_{k\alpha\sigma}) g_{i\sigma}^r$ , we have  $G_{\sigma\sigma'}^{(2)}$  in the form of

$$\begin{aligned} (\omega - \varepsilon_{c\sigma} - U) G_{\sigma\sigma'}^{(2)} = & n_{\bar{\sigma}} \delta_{\sigma\sigma'} + (\Sigma_{1\sigma} + \Sigma_{2\bar{\sigma}} + \Sigma_{3\bar{\sigma}} + \Sigma_{4\sigma} + \Sigma_{5\bar{\sigma}} \\ & + \Sigma_{6\sigma}) G_{\sigma\sigma'}^{(2)} + (\bar{\sigma} \Sigma_{3\bar{\sigma}} + \sigma \Sigma_{4\sigma}) G_{\bar{\sigma}\sigma'}^{(2)} - (\Sigma_{3\bar{\sigma}}^f + \Sigma_{4\sigma}^f + \Sigma_{5\bar{\sigma}}^f \\ & + \Sigma_{6\sigma}^f) G_{\sigma\sigma'}^R - (\sigma \Sigma_{1\sigma}^f + \bar{\sigma} \Sigma_{2\bar{\sigma}}^f + \bar{\sigma} \Sigma_{3\bar{\sigma}}^f + \sigma \Sigma_{4\sigma}^f) G_{\bar{\sigma}\sigma'}^R. \end{aligned} \quad (19)$$

Making the truncation as above, the equation for  $G_{\sigma\sigma'}^{(2)}$  is close. It now only involves the Green's functions  $G_{\sigma\sigma'}^{(2)}$ ,  $G_{\bar{\sigma}\sigma'}^{(2)}$ ,  $G_{\sigma\sigma'}^R$  and  $G_{\bar{\sigma}\sigma'}^R$ . One can solve them self-consistently. With the notations of  $\hat{\varepsilon}_{c\sigma} = \begin{pmatrix} \varepsilon_{c\sigma} & 0 \\ 0 & \varepsilon_{c\bar{\sigma}} \end{pmatrix}$ ,  $\hat{\mathbf{n}} = \begin{pmatrix} n_{\bar{\sigma}} & 0 \\ 0 & n_{\sigma} \end{pmatrix}$ ,

$$\hat{\Sigma}_0 = \begin{pmatrix} \Sigma_{1\uparrow} + \Sigma_{2\downarrow} & \Sigma_{1\downarrow} - \Sigma_{2\uparrow} \\ \Sigma_{1\downarrow} - \Sigma_{2\uparrow} & \Sigma_{1\uparrow} + \Sigma_{2\downarrow} \end{pmatrix}, \quad \hat{\Sigma}_1 = \begin{pmatrix} \Sigma_{5\downarrow}^f + \Sigma_{6\uparrow}^f & \Sigma_{1\uparrow}^f - \Sigma_{2\downarrow}^f \\ \Sigma_{1\uparrow}^f - \Sigma_{2\downarrow}^f & \Sigma_{5\uparrow}^f + \Sigma_{6\downarrow}^f \end{pmatrix},$$

$$\hat{\Sigma}_2 = \begin{pmatrix} \Sigma_{1\uparrow} + \Sigma_{2\downarrow} + \Sigma_{5\downarrow} + \Sigma_{6\uparrow} & 0 \\ 0 & \Sigma_{1\downarrow} + \Sigma_{2\uparrow} + \Sigma_{5\uparrow} + \Sigma_{6\downarrow} \end{pmatrix}, \text{ and}$$

$$\hat{\Sigma}_3^{(f)} = \begin{pmatrix} \Sigma_{3\uparrow}^{(f)} + \Sigma_{4\downarrow}^{(f)} & \Sigma_{3\uparrow}^{(f)} - \Sigma_{4\downarrow}^{(f)} \\ \Sigma_{3\uparrow}^{(f)} - \Sigma_{4\downarrow}^{(f)} & \Sigma_{3\uparrow}^{(f)} + \Sigma_{4\downarrow}^{(f)} \end{pmatrix}, \text{ defining } \hat{\Sigma}_4 = \omega \hat{\mathbf{1}} - \hat{\varepsilon}_{c\sigma} - U \hat{\mathbf{1}} - \hat{\Sigma}_2 - \hat{\Sigma}_3, \text{ one}$$

can write the Green's function  $G^R$  in a compact form as below

$$\hat{G}^R = [\omega \hat{\mathbf{1}} - \hat{\varepsilon}_{c\sigma} - \hat{\Sigma}_0 + U \hat{\Sigma}_4^{-1} (\hat{\Sigma}_3^{(f)} + \hat{\Sigma}_1)]^{-1} (\hat{\mathbf{1}} + U \hat{\mathbf{n}} \hat{\Sigma}_4^{-1}). \quad (20)$$

In the infinite  $U$  limit, we recover the result in Refs. [9,18],

$$\hat{G}^R = (\omega \hat{\mathbf{1}} - \hat{\varepsilon}_{c\sigma} - \hat{\Sigma}_0 - \hat{\Sigma}_1)^{-1} (\hat{\mathbf{1}} - \hat{\mathbf{n}}). \quad (21)$$

To determine the lesser Green's function of the dot  $\mathbf{G}^<$ , we use the Ng's ansatz[21] in our case. The interaction lesser and greater self-energies are assumed to be of the form  $\Sigma^{<,>} = \Sigma_0^{<,>} \mathbf{A}$ , where  $\mathbf{A}$  is a matrix to be determined

by the condition of  $\Sigma^{<-\Sigma^>}=\Sigma^R-\Sigma^A$ . This ansatz is exact in the noninteracting limit ( $U=0$ ) and guarantees automatically the current conservation law. As a result one obtains  $\Sigma^{<}=\Sigma_0^{<}[\Sigma_0^R-\Sigma_0^A]^{-1}[\Sigma^R-\Sigma^A]$ . Using this results,  $\mathbf{G}^{<}$  can be obtained by Keldysh equation  $\mathbf{G}^{<}=\mathbf{G}^R\Sigma^{<}\mathbf{G}^A$ . Substituting the expressions of the Green's functions of quantum dot into Eq. (6) and defining  $\bar{\Sigma}^{<}=\mathbf{\Gamma}^R(\mathbf{\Gamma}^L+\mathbf{\Gamma}^R)^{-1}(\Sigma^R-\Sigma^A)$ , one obtains an expression of the tunnelling current

$$J = \frac{ie}{\hbar} \int \frac{d\epsilon}{2\pi} \text{Tr}[\mathbf{\Gamma}^L \mathbf{G}^R \bar{\Sigma}^{<} \mathbf{G}^A] [f_L(\epsilon) - f_R(\epsilon)]. \quad (22)$$

This expression generalizes the well known current formula to the spin-dependent Anderson model with additional spin-flip relaxation and allows one to describe the coherent spin transport through an interacting quantum dot coupled to magnetic electrodes.

### 3 Numerical results

In this section, we will present the numerical results of spin-dependent DOS and conductance. For simplicity, we neglect the energy dependence of the tunnelling matrix elements and consider parallel and antiparallel configurations. If the magnetic moments in the electrodes are parallel, the spin-majority electrons are assumed to be spin-up and the spin-minority electrons are spin-down. In the antiparallel configuration, the magnetization of the left electrode is up and the magnetization of the right electrode is down. With these assumptions the coherent spin transport parameters can be conveniently expressed by introducing magnetic polarization factors  $p_L$  and  $p_R$  for the left and right barriers, respectively. Therefore,  $\Gamma_{\uparrow(\downarrow)}^L = \Gamma_0(1 \pm p_L)$  and  $\Gamma_{\uparrow(\downarrow)}^R = \alpha\Gamma_0(1 \pm p_R)$  are for the parallel configuration, and  $\Gamma_{\uparrow(\downarrow)}^L = \Gamma_0(1 \pm p_L)$ ,  $\Gamma_{\uparrow(\downarrow)}^R = \alpha\Gamma_0(1 \mp p_R)$  for the antiparallel configuration.  $\Gamma_0$  describes the coupling between the quantum dot and the left electrode without internal magnetization. We express all parameters in the unit of  $\Gamma_0$  in the following calculation.  $\alpha$  denotes tunnel asymmetric factor of the left and right barriers. In this work, we assume the symmetric barriers, i.e.,  $\alpha=1$ ,  $p_L=p_R=p$ .

The spin-resolved DOS in the dot are calculated via the relation  $\rho_{\uparrow(\downarrow)} = -1/\pi \text{Im}\{G_{\uparrow\uparrow}^R \mp G_{\uparrow\downarrow}^R \mp G_{\downarrow\uparrow}^R + G_{\downarrow\downarrow}^R\}$ . The Kondo resonance for each spin is clearly manifested by the peak at  $\omega=0$  in the DOS for both parallel and antiparallel configurations. However, the shape of the peak is sensitive to the magnetic configurations of the electrodes. As observed from Fig. 1(a), in the parallel configuration the spin-up DOS (solid line in Fig. 1(a)) is dramatically different from that of spin-down (dotted line in Fig. 1(a)) in the infinite  $U$  limit, while in the antiparallel configuration the DOS for spin-up and spin-down are

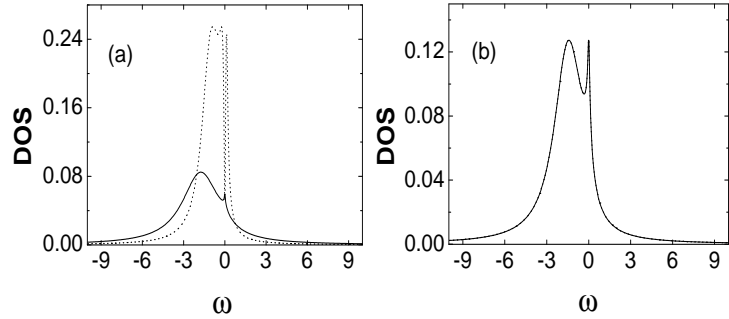


Fig. 1. Density of states in the parallel (a) and antiparallel (b) configurations in the infinite  $U$  limit, the solid line is for spin-up and the dotted line is for spin-down. Here  $\varepsilon_d = -2$ ,  $K_B T = 0.001$ ,  $p = 0.5$ ,  $R = 0$ .

identical, see Fig. 1(b). In Fig. 1(b) the Kondo peak for spin-up and spin-down is not affected by the magnitude of magnetic polarizations  $p$ . As we know that the spin current of electrons through the antiparallel configuration cannot be polarized, whereas can be polarized through the parallel configuration[22]. Therefore, the DOS for spin-up is different from that of spin-down in the parallel configuration and is the same as that of spin-down in the antiparallel configuration.

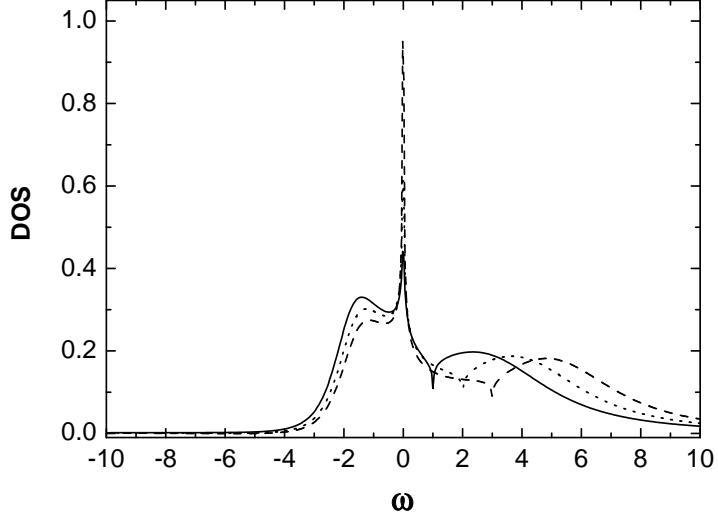


Fig. 2. Spin-up density of states in the antiparallel configuration for  $U=5$  (solid line), 6 (dotted line), and 7 (dashed line). Here  $R=0$ , the other parameters are the same as in Fig.1.

In the limited Coulomb repulsion  $U$ , the spin-up DOS in the antiparallel configuration are plotted in Fig. 2. It can be seen from Fig. 2, there are two broad maxima in DOS, which are centered at the positions of the dot level  $\varepsilon_d$  and  $\varepsilon_d + U$ , respectively. However, for infinite  $U$  limit case, as shown in Fig. 1, there is only one broad maximum. It is consistent with physical intuition since for the infinite  $U$  there is only one level in the dot but are two levels for the finite  $U$ . This result agrees with other authors' work[18,12]. The Kondo

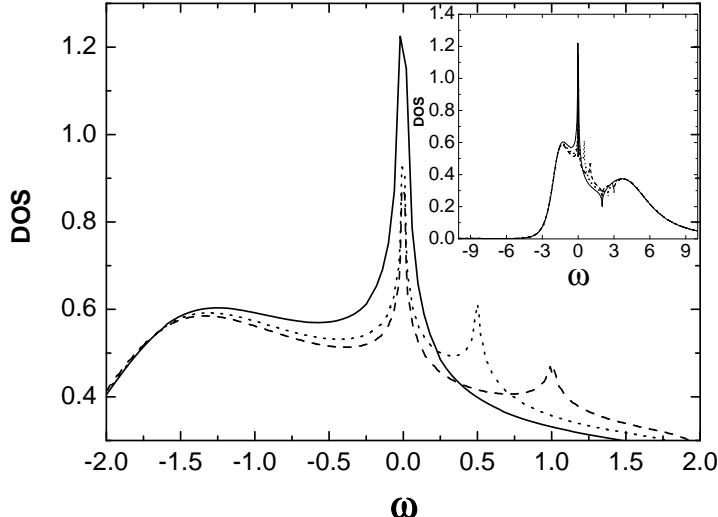


Fig. 3. Total density of states in the antiparallel configuration with  $v=0$  (solid line),  $0.5$  (dotted line), and  $1$  (dashed line), respectively. Here  $U=6$ , the other parameters are the same as in Fig.1.

peak in DOS is exactly located at the Fermi level, see the sharp peak in Fig. 2. This is the equilibrium situation (the applied bias is set to be zero). When the voltage is applied (the left chemical potential is different from that of the right), the Kondo peak splits into two peaks with lower intensities at positions of the left and the right chemical potentials. This behavior is shown in Fig. 3 for three different values of the bias voltages. As the bias voltage increases the splitting of the Kondo peak becomes wider and is equal to the difference of the bias. The Fig. 3 is plotted in a narrow energy range around the Kondo peak, the inset of the figure gives a wider view in energy. It is evident that the peaks occur at the Fermi levels of the two electrodes. The solid line is for zero bias, there is only one peak at  $\omega = 0$ . The dotted line is for bias  $v=0.5$  and the second peak appears at the position  $\omega = 0.5$ . The dashed line is for  $v=1$ , the splitting peak is at  $\omega = 1$ . This behavior is in accordance with other results[23,24,25].

The interesting feature in this work is that there exists a splitting due to the spin-flip transition processes. In the preceding discussions there is always a Kondo peak at the energy  $\omega = 0$ . However, if we set spin-flip parameter  $R$  not to be zero, as shown in Fig. 4 for the DOS of spin-up in the antiparallel configuration, the original Kondo peak splits into two peaks. The two peaks appear at the positions of  $\omega = \pm R$ , respectively, and the original peak at  $\omega = 0$  disappears. In Fig. 4 the solid line is plotted without spin-flip transition, the dotted line is for spin-flip transition parameter  $R = 0.2$  and the dashed line is  $R = 0.5$ . The inset in Fig. 4 is also a global view of the Kondo effect. The splitting is due to the coupling of spin-flip transition processes between the dot and the magnetic electrodes and can be expressed by the high order self-energy.

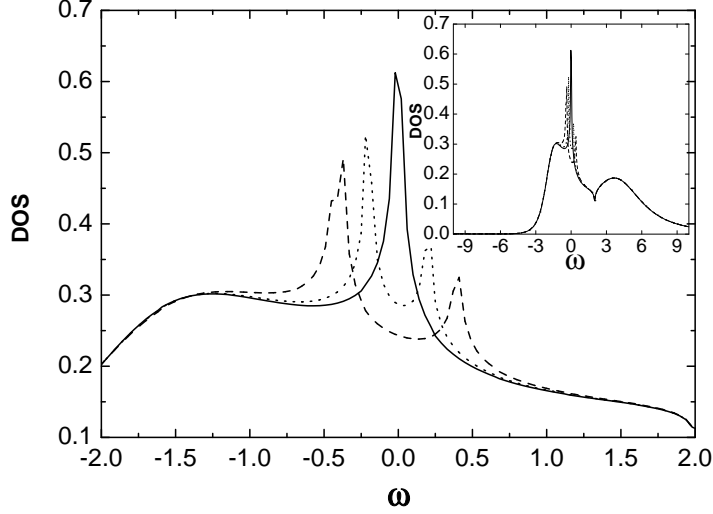


Fig. 4. Spin-up density of states in the antiparallel configuration with  $R=0$  (solid line), 0.2 (dotted line), and 0.5 (dashed line), respectively. Here  $U=6$ , the other parameters are the same as in Fig.1.

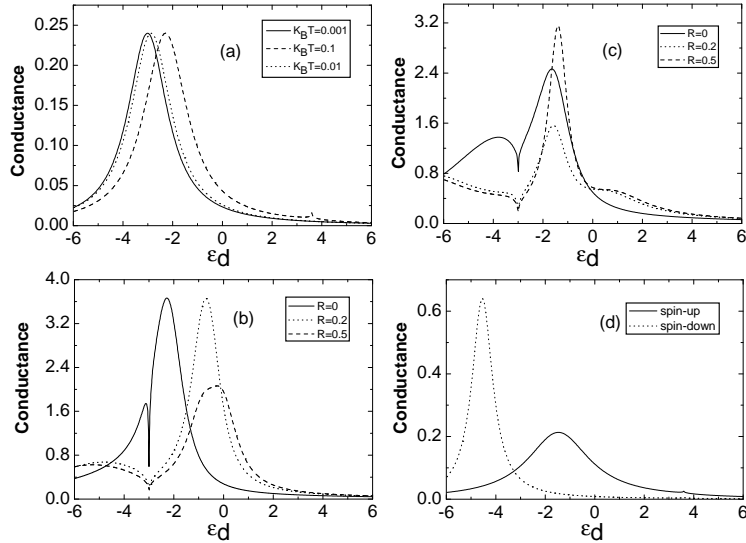


Fig. 5. The conductance in the antiparallel and antiparallel configurations. (a) in the antiparallel configuration for the infinite  $U$  limit and different temperatures. The spin-flip parameter  $R=0$ . (b) in the antiparallel configuration for different  $R$ , here  $U=6$  and  $K_B T=0.001$ . (c) in the parallel configuration for different  $R$ , the other parameters are the same as in (b). (d) the conductance in the parallel configuration for the spin-up and spin-down, respectively,  $K_B T=0.001$ , the other parameters are the same as in (a).

In Fig. 5, we show the linear response conductance as a function of energy  $\varepsilon_d$  of the dot in the parallel and antiparallel configurations. In the antiparallel configuration the conductance is similar to the normal case, i.e., the Kondo effect broadens the conductance peak, see Fig. 5(a). The peaks are similar in shape for different temperatures. They only shift a little to each other. As temperature increases the peak shifts to the higher energy. This is caused

by the shift of the Fermi energy for different temperatures. Due to the DOS for spin-up and spin-down are the same in the antiparallel configuration, as seen in Fig. 1, the conductances for spin-up and spin-down are overlapped in this configuration. However, when  $U$  is finite, for instance  $U=6$ , the conductance of spin-up differs to that of spin-down, see solid line in Fig. 5(b). If the spin-flip process on the quantum dot is involved, this shift becomes more dramatically, see the dotted line and dashed line in Fig. 5(b). For a large value of  $R$  the amplitude of conductance is small. In the parallel configuration the conductances for spin-up and spin-down are different[22], see Fig. 5(d), the resonance of spin-up conductance (solid line) has an apparent shift to the spin-down (dotted line) due to different densities of states for them [see Fig. 1(a)]. The existence of the spin-flip transition  $R$  reduces the spin-down conductance under the finite  $U$  condition, see Fig. 5(c). Increasing the value of  $R$  the spin-up conductance becomes higher and the spin-down conductance becomes lower. This effect is caused by the correlation between the dot and the ferromagnetic electrodes. For a large enough  $R$  the peak of conductance of spin-down is suppressed and the spin-up peak is enhanced. We expect this result may be important in the exploiting the spin-filter devices.

## 4 Conclusion

Using the Anderson model, we study the Kondo effect in the ferromagnetic-quantum dot-ferromagnetic system. We find that the spin-dependent transport in such a system is sensitive to the alignment of the magnetic moments in electrodes. Due to the external applied bias or the spin-flip process on the dot, the original Kondo peak splits into two peaks. The conductances in the parallel and antiparallel magnetic configurations are affected by the spin-flip transition and the Coulomb repulsion on the dot. We expect that the effects can be useful to realize the high spin polarization devices.

## Acknowledgments

This work was supported by NSFC Grant No. 10274069, 60471052, 10225419, 10347003; the Zhejiang Provincial Natural Foundation M603193.

## References

### References

- [1] A. C. Hewson, *The Kondo Problem to Heavy Fermions* (Cambridge University Press, Cambridge, 1993).
- [2] L. I. Glazman and M. E. Raikn, JETP Lett. **47**, 452 (1998).
- [3] S. Sasaki *et al.*, Nature (London) **405**, 764 (2000).
- [4] W. G. van der Wiel *et al.*, Science **289** 2105 (2000).
- [5] J. Gores *et al.*, Phys. Rev. B **62**, 2188 (2000).
- [6] N. S. Wingreen and Y. Meir, Phys. Rev. B **48**, 11040 (1994).
- [7] J. Barnaś and A. Fert, Phys. Rev. Lett. **80** 1058 (1998).
- [8] J. Barnaś *et al.*, Phys. Rev. B **62** 12363 (2000).
- [9] Y. Meir, N. S. Wingreen, and P. A. Lee, Phys. Rev. Lett. **70**, 2601 (1993).
- [10] Y. Meir, N. S. Wingreen, and P. A. Lee, Phys. Rev. Lett. **66**, 3048 (1991).
- [11] C. Niu, D. L. lin, and T. H. Lin, J. Phys.: Condens. Matter **11**, 1511 (1991).
- [12] N. Sergueev, Q. F. Sun, H. Guo, B. G. Wang, and J. Wang, Phys. Rev. B **65**, 165303 (2002).
- [13] A. P. Jauho, N. S. Wingreen, and Y. Meir, Phys. Rev. B. **50**, 5528 (1994).
- [14] A. K. Zhuravlev *et al.*, Phys. Rev. Lett. **93**, 236403 (2004).
- [15] Domenico Giuliano, Adele Naddeo, and Artuto Tagliacozzo, J. Phys.: Condens. Matter **16**, s1453 (2004).
- [16] Yasuhiro Utsumi *et al.*, cond-mat/0501172.
- [17] A. Kogan *et al.*, Phys. Rev. Lett. **93**, 166602 (2004).
- [18] Ping Zhang, Qi-Kun Xue, Yupeng Wang, and X. C. Xie, Phys. Rev. Lett. **89**, 286803 (2002).
- [19] Mahn-Soo Choi, David Sanchez, and Rosa Lopez, Phys. Rev. Lett. **92**, 056601 (2004).
- [20] C. Lacroix, J. Phys. F: Met. Phys. **11**, 2389 (1981).
- [21] T. K. Ng, Phys. Rev. Lett. **76**, 487 (1996).
- [22] V. N. Dobrovolsky, D. I. Sheka, B. V. Chernyachuk, Surface Science **397**, 333 (1998).

- [23] J. Martinek, Y. Utsumi, H. Imamura, J. Barnaś, S. Maekawa, J. König, and G. Schön, Phys. Rev. Lett. **91**, 127203 (2003).
- [24] M. Krawiec and K. I. Wysokiński, Phys. Rev. B **66**, 165408 (2002).
- [25] T. A. Costi, Phys. Rev. Lett. **85**, 1722 (2000); Phys. Rev. B. 64, 241310 (2001).